

Cranial anatomy of the giant anteater from northwestern Venezuela (*Myrmecophaga tridactyla artata*, Pilosa: Myrmecophagidae)

Anatomía craneana del oso hormiguero gigante del noroccidente de Venezuela
 (*Myrmecophaga tridactyla artata*, Pilosa: Myrmecophagidae)

Juan D. Carrillo^{1,2*}, Luis E. Sibira³ & Tito R. Barros³

¹Department of Biology, University of Fribourg, and Swiss Institute of Bioinformatics, 1700, Fribourg, Switzerland

²Gothenburg Global Biodiversity Centre, SE-405 30, Gothenburg, Sweden

³Museo de Biología, Facultad Experimental de Ciencias, Universidad del Zulia, Maracaibo, Venezuela.

Correspondence: juan.carrillo@unifr.ch

(Recibido: 23-12-2021 / Aceptado: 06-07-2022 / En línea: 30-09-2022)

ABSTRACT

The giant anteater (*Myrmecophaga tridactyla*) has a wide geographical distribution in Central and South America. Three subspecies are tentatively recognized for populations in Central America and west of the northern Andes (*M. tridactyla centralis* Lyon, 1906), northern Colombia and northwestern Venezuela (*M. tridactyla artata* Osgood, 1912), and the rest of South America (*M. tridactyla tridactyla* Linnaeus, 1758). *Myrmecophaga tridactyla artata* is the less known of the three subspecies, and few specimens are deposited in zoological collections. Recent collecting efforts of specimens from northwestern Venezuela allow us to better characterize this morphotype and evaluate morphological differences with the other two subspecies. We found that adult specimens of *M. t. artata* show smaller cranial dimensions in comparison with *M. t. centralis* and *M. t. tridactyla*. We document a higher morphological variation than previously recognized in the cranial sutures that have been hypothesized to differentiate the subspecies. Although *M. t. artata* shows smaller cranial dimensions than *M. t. centralis* and *M. t. tridactyla*, additional data integrating information from the genetic variation and other morphological regions is required to further evaluate the morphological and genetic differences of the three recognized subspecies. The recently collected specimens of *M. t. artata* studied herein shed light on the cranial morphological variation and overlap among the three recognized subspecies of the giant anteater.

Keywords: Xenarthra, crania, South America, tropics, morphology.

RESUMEN

El oso hormiguero gigante (*Myrmecophaga tridactyla*) tiene una amplia distribución geográfica en Centro y Suramérica. Tres subespecies son reconocidas para las poblaciones de Centroamérica y el oeste del norte de los Andes (*M. tridactyla centralis* Lyon, 1906), el norte de Colombia y el noroeste de Venezuela (*M. tridactyla artata* Osgood, 1912), y el resto de Sudamérica (*M. tridactyla tridactyla* Linnaeus, 1758). *Myrmecophaga t. artata* es la menos conocida de las tres subespecies, y hay pocos ejemplares depositados en colecciones zoológicas. Recientes esfuerzos de colección de ejemplares atropellados en el noroeste de Venezuela nos permiten caracterizar mejor este morfotipo y evaluar las diferencias morfológicas con las otras dos subespecies. Los individuos adultos de *M. t. artata* tienen unas dimensiones craneanas menores en comparación con *M. t. centralis* y *M. t. tridactyla*. Adicionalmente, documentamos una variación morfológica mayor que la reconocida anteriormente en las suturas craneales que se han propuesto para diferenciar las subespecies. Aunque *M. t. artata* muestra unas dimensiones craneanas más pequeñas que *M. t. centralis* y *M. t. tridactyla*, se necesitan datos adicionales que integren

la información de la variación genética y de otras regiones morfológicas para evaluar más a fondo las diferencias morfológicas y genéticas de las tres subespecies reconocidas. Los ejemplares de *M. t. artata* recientemente recolectados y estudiados aportan nueva información sobre la variación de la anatomía craneana entre las tres subespecies reconocidas del oso hormiguero gigante.

Palabras clave: Xenarthra, cráneo, Suramérica, trópico, morfología.

INTRODUCTION

The giant anteater (*Myrmecophaga tridactyla* Linnaeus, 1758) is the largest extant representative of the order Pilosa (Gaudin *et al.* 2018). *M. tridactyla* is terrestrial and inhabits a wide range of habitats, from wet rainforests to dry savannahs (Rodrigues *et al.* 2008). The skull of giant anteaters is characterized by several adaptations to myrmecophagy (ant- and termite eating; Redford 1987) such as long and edentulous snouts, protractile tongues, and reduced masticatory apparatus (Naples 1999, Casali *et al.* 2017, Ferreira-Cardoso *et al.* 2020b). It is hypothesized that the giant anteater originated from the extinct taxon *Neotamandua* (Rovereto 1914, Hirschfeld 1976), at about 8.1 million years ago (Ma) (Casali *et al.* 2020). Among the living taxa, the giant anteater is closely related to the genus *Tamandua* Gray 1825 (*Tamandua mexicana* and *Tamandua tetradactyla*) with an estimate time of divergence at about 13 Ma (12.7 Ma estimated by Gibb *et al.* [2016] and 13.6 Ma estimated by Casali *et al.* [2020]).

Several studies focused on the phenotypic variation among widely distributed myrmecophagous mammals (Ferreira-Cardoso *et al.* 2020a), including tamanduas (Reeve 1940, Wetzel 1975) and the silky anteaters (genus *Cyclopes* Gray 1821) (Miranda *et al.* 2018). Reeve (1940) proposed the existence of several subspecies within *Tamandua tetradactyla* and *Tamandua mexicana* based of internal and external morphological traits, while Miranda *et al.* (2018) showed that *Cyclopes* is constituted of at least seven cryptic species.

Similar to other pilosans (Hayssen 2011, Navarrete & Ortega 2011, Miranda *et al.* 2018), the giant anteater is widely geographically distributed, spanning from Central America to Southern Brazil (Fig. 1). Gardner (2007) and Gaudin *et al.* (2018) tentatively recognized three subspecies for populations in central America, and west of the Andes in Colombia and Ecuador (*Myrmecophaga tridactyla centralis* Lyon 1906), northern Colombia and northwestern Venezuela (*Myrmecophaga tridactyla artata* Osgood 1912) (Pittier & Tate 1932, Linares 1998), and rest of South America (*Myrmecophaga tridactyla tridactyla*) (Fig. 1). *M. t. centralis* was described originally as a new species by Lyon (1906) based on differences of the sutures

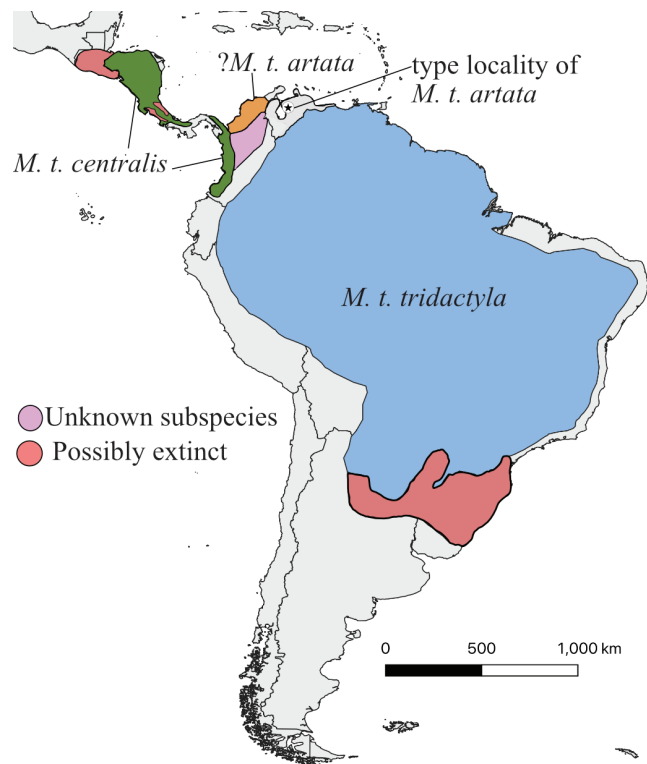


Figure 1. Geographic distribution of *Myrmecophaga tridactyla* showing the distribution of the three subspecies (Gardner 2007, Gaudin *et al.* 2018). *M. t. centralis* (green), *M. t. artata* (orange), and *M. t. tridactyla* (light blue). The range distribution of *M. t. artata* and *M. t. tridactyla* in Venezuela was modified from Gaudin *et al.* (2018) and Linares (1998). The type locality of *M. t. artata* (Empalado savannas; Osgood 1912) is indicated by the black star. The new specimens of *M. t. artata* studied in this work come from nearby the type locality (Supplementary Table 1). Geographic range map distribution of *M. tridactyla* was modified from Miranda *et al.* (2014). The light purple represents the extension of the distribution range in Colombia following Chacón Pacheco *et al.* (2017).

between the nasals and the frontals, and the squamosal and sphenoid. The description of *M. t. centralis* was based on a juvenile specimen from Costa Rica, but some of its characteristics are observed also in adults from Honduras (Mérida Colindres & Cruz Dias 2014). *M. t. artata* was

described by Osgood (1912) based mainly on a narrower rostrum (narrower nasals and less expanded maxillaries) than the two other subspecies. Given its restricted distribution, the populations from northern Colombia and north-western Venezuela (tentatively designated as the subspecies *M. t. artata*; Linares 1998, Gaudin *et al.* 2018) are poorly known. During a period of five years (2008–2013), one of the authors (TRB) has collected several individuals in northwestern Venezuela (Falcón and Zulia states), all of which were road-killed in a section of paved road of 81 km, from the bifurcation towards Los Puertos de Altagracia (10.581033, -71.473431) until Santa Cruz (10.877166, -70.881389). In this work we study the crano-mandibular anatomy of the giant anteater from north-western Venezuela (*M. t. artata*) with the aim to better characterize this morphotype and evaluate morphological differences with the other two tentative subspecies (*M. t. centralis* and *M. t. tridactyla*).

MATERIALS AND METHODS

We measured 65 dry skulls of museum specimens of *Myrmecophaga tridactyla* collected across different localities in Central and South America (Carrillo *et al.* 2022; Supplementary Table 1). The specimens represent the three tentatively recognized subspecies, *M. t. centralis* (2 specimens), *M. t. artata* (10 specimens) and *M. t. tridactyla* (37 specimens), and zoo animals (6 specimens). Nine specimens had no locality information (Supplementary Table 1). In addition, we included one specimen of *M. t. centralis* with the measurements reported by (Mérida Colindres & Cruz Dias 2014). For the statistical analyses to compare the three tentatively recognised subspecies, we excluded the zoo specimens and specimens without locality information.

We took the following 14 linear measurements (Fig. 2):
(1) Skull length (SL), from the most dorso-caudal point

Table 1. Principal Component eigenvalues, variables correlations and contribution to the first five dimensions. Dim = dimension; var. = variance; cor = correlation; contr = contribution. The numbers and abbreviations of the variables correspond to the ones described in the text.

Variance	Dim 1	Dim 2	Dim 3	Dim 4	Dim 5	Dim 6	Dim 7	Dim 8	Dim 9	Dim 10
	7.1	1.64	1.14	0.82	0.82	0.64	0.52	0.47	0.28	0.25
% of var.	50.71	11.68	8.12	5.87	5.86	4.59	3.72	3.39	2.02	1.77
Cumulative % of var.	50.71	62.39	70.51	76.38	82.24	86.83	90.55	93.94	95.96	97.74
Variables	Dim 1		Dim 2		Dim 3		Dim 4		Dim 5	
	cor	contr								
1. SL	0.93	12.26	0.04	0.08	-0.06	0.32	0.11	1.48	-0.09	0.97
2. CL	0.96	13.05	-0.02	0.01	0.05	0.22	0.04	0.19	-0.1	1.14
3. WS	0.79	8.81	-0.22	3	-0.28	6.94	0.02	0.07	-0.15	2.83
4. AW	0.33	1.51	-0.83	42.57	0.13	1.54	0.13	1.98	-0.22	5.67
5. LW	0.69	6.73	0.1	0.65	-0.39	13.44	0.33	13.14	0.12	1.89
6. ML	0.93	12.18	0.07	0.31	0.09	0.66	-0.04	0.24	-0.13	1.98
7. OW	0.76	8.14	-0.31	5.97	0.16	2.2	-0.18	4.04	-0.08	0.78
8. OCW	0.7	6.89	-0.22	2.88	0.02	0.03	-0.09	0.89	0.36	15.82
9. FMH	0.25	0.9	0.57	19.8	0.45	17.82	0.45	24.58	-0.08	0.74
10. CH	0.62	5.43	0.22	2.92	0.43	16.03	0.11	1.51	0.06	0.37
11. PL	0.56	4.37	-0.04	0.08	0.16	2.12	-0.16	3.13	0.7	59.27
12. PW	0.47	3.07	0.37	8.47	-0.66	37.91	0.03	0.08	0.03	0.13
13. VL	0.96	13.09	0.02	0.02	0.05	0.18	0.02	0.07	-0.09	0.96
14. LD	0.5	3.54	0.47	13.24	0.08	0.59	-0.63	48.62	-0.25	7.45

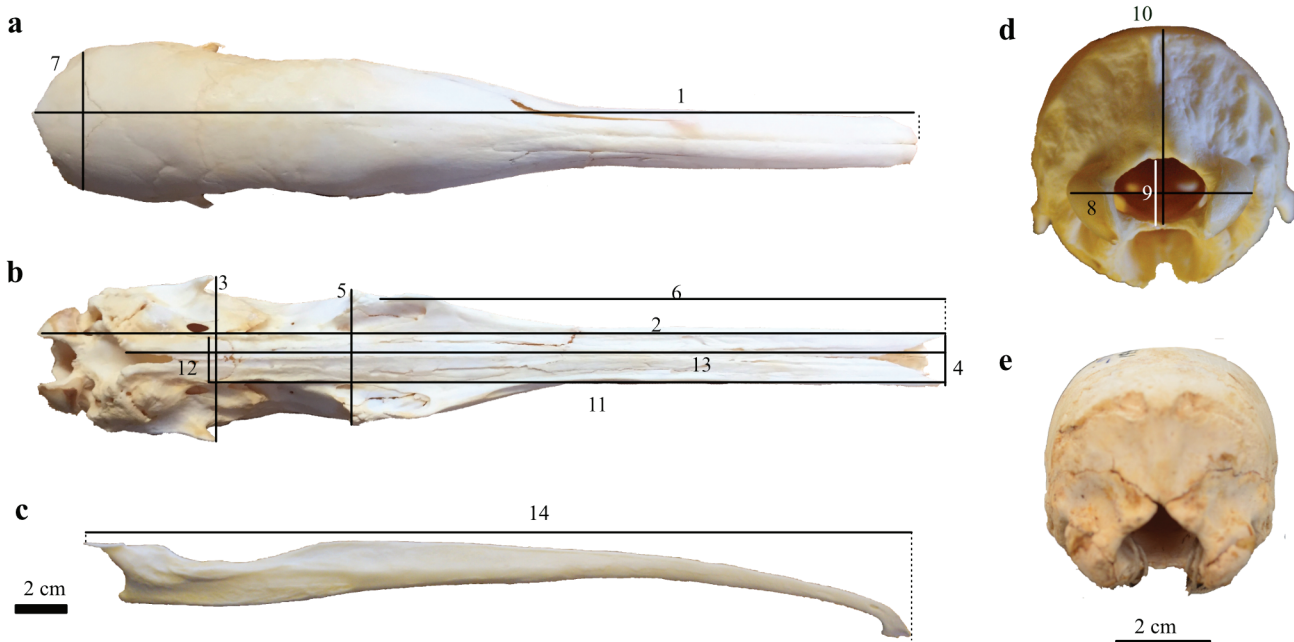


Figure 2. Linear measurements used in this study. Measurements are illustrated in a skull of *M. t. artata* (MBLUZ-0249) in dorsal view (a), ventral view (b), and caudal view (c). The numbers correspond to the list of measurements described in materials and methods. d. Caudal view of the only subadult specimen (NRM 586631) in the sample (as indicated by supraoccipital-exoccipital suture not fully closed), referred to *M. t. tridactyla*.

of the occipital to the most rostral point of the nasal; (2) Condylobasal length (CL), from the most caudal point of the occipital condyle to the most rostral point of the maxilla. (3) Width between the squamosal processes (WS), distance between the most rostro-lateral point of the squamosal processes of the temporal; (4) Anterior width (AW), the distance between the most rostral point of the maxillas; (5) Lacrimal width (LW), the distance between the most lateral point of the lacrimals; (6) Maxilla length (ML), from the most caudal to the most rostral point of the maxilla; (7) Occipital width (OW), the distance between the most caudal point of the occipital-parietal sutures; (8) Occipital condyles width (OCW), the distance between the most lateral points of the occipital condyles; (9) Foramen magnum height (FMH), dorso-ventral height of the foramen magnum; (10) Cranial height (CH), from the most ventral point of the foramen magnum to the most dorsal point of the occipital; (11) Palatal length (PL), from the most caudal point of the palatine to the most rostral point of the maxilla; (12) Palatal width (PW), the distance between the most caudo-lateral point of the palatines; (13) Ventral length (VL), from the most caudal point of the sphenoid to the most rostral point of the maxilla; (14) Length of dentary (LD), from the most caudal point of the mandibular condyle to

the most rostral point of the mandibular symphysis. All specimens measured are adults (as indicated by the closed supraoccipital-exoccipital suture), except for one subadult individual representing *M. t. tridactyla* (NRM 586631), for which this suture is not completely closed (Fig. 2e). We used a calliper to the nearest 0.1 mm and a metric tape for large measurements (>15 cm).

Data were collected from specimens from the following institutions: ZMUZH, Zoologisches Museum der Universität Zürich; MBLUZ, Museo de Biología de la Universidad de Zulia, Maracaibo; MNHN, Muséum national d'Histoire naturelle, Paris; ZMB, Museum für Naturkunde, Berlin; ZSM Zoologisches Staatssammlung, München; ICN, Instituto de Ciencias Naturales, Bogotá; NRM, Naturhistoriska riksmuseet, Stockholm; GNM, Göteborgs Naturhistorika Museum Gothenburg; and COSEM-MAS, Instituto Commemorativo Gorgas de Ciencias de la Salud, Panama.

The following analyses were performed on the sample of specimens that could be assigned to one of the three subspecies ($n=50$). We fitted a linear regression of the skull length and lacrimal width (chosen as a measurement to represent relative skull width). In addition, to compare the relative width and length of the skull among the three subspecies, we estimated the ratio of lacrimal width / skull

length. We also performed a principal component analysis (PCA) (Dryden & Mardia 1993) on the 14 skull measurements in order to visualize the skull shape variation. We used the missMDA package (Josse & Husson 2016) to impute some missing values, because not all the 14 measurements could be taken in all the specimens studied. The missing value imputation uses the regularized iterative PCA algorithm which considers the similarities of observations and the relationships of the variables. In brief, the algorithm substitute missing values with initial values (e.g., mean of the variable with no missing entries), then performs a PCA and use the fitted matrix to defined new imputed data (the observed values remain the same, but the missing values are replaced by the fitter values). This process is repeated until the change of the imputed matrix

is below a pre-defined threshold (Josse & Husson 2016). We did the PCA using the FactoMineR package (Husson *et al.* 2020). All analyses and plots were made in R (R Core Team 2021).

RESULTS

The bivariate plot of skull length and lacrimal width shows a positive relationship between the two variables (adjusted $R^2 = 0.48$, p-value < 0.001). Overall, the specimens representing *M. t. artata* tend to have shorter and narrower skulls in comparison with specimens representing *M. t. tridactyla*, whereas the three specimens of *M. t. centralis* show intermediate values of skull length (Fig. 3a). When comparing the relative width and length of the

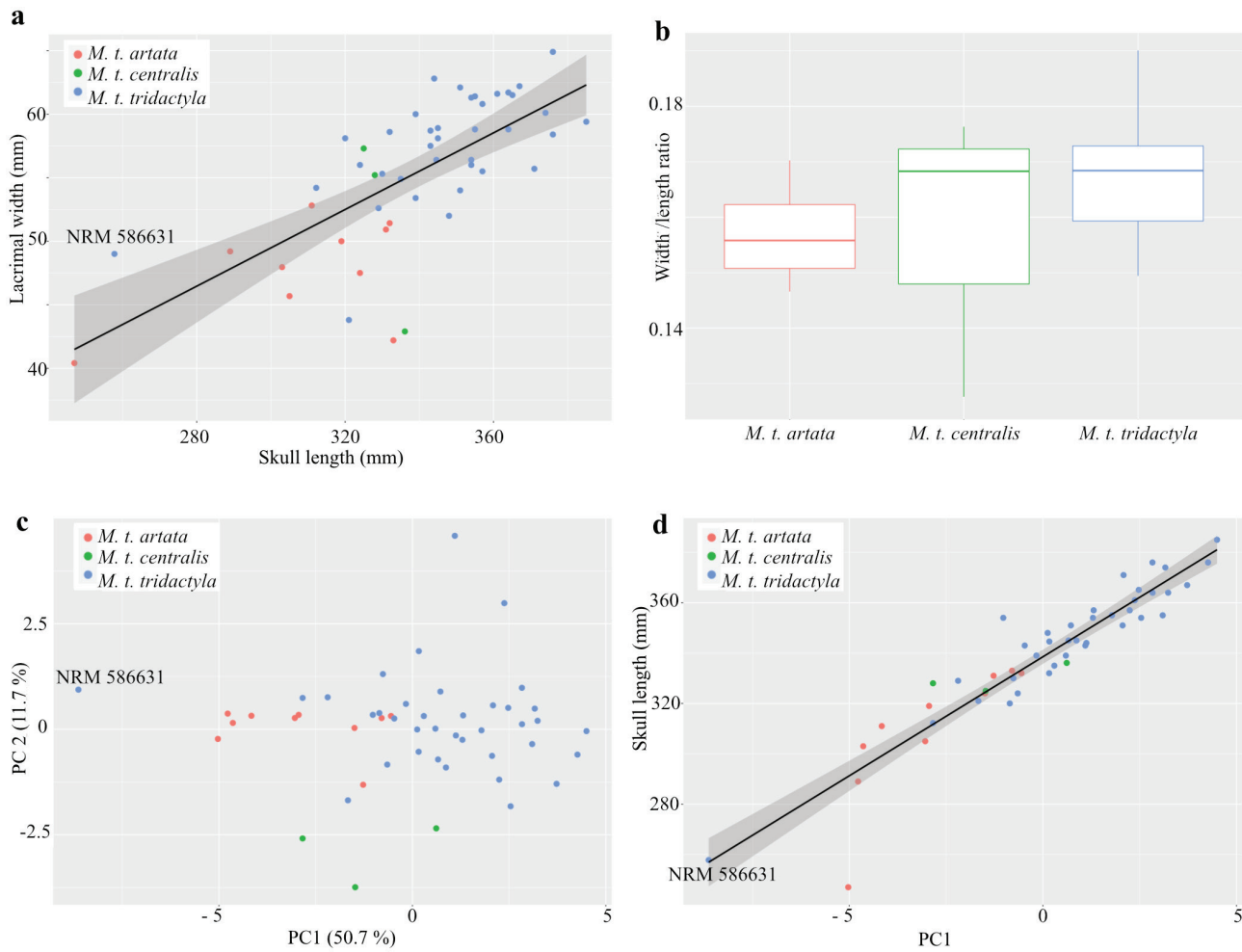


Figure 3. Skull dimensions and morphospace occupation of the three recognized subspecies of *Myrmecophaga tridactyla*: *M. t. centralis* (green), *M. t. artata* (red), *M. t. tridactyla* (blue). The text indicates the position of a subadult specimen of *M. t. tridactyla* (NRM 586631). **a.** Bivariate plot of the skull length and lacrimal width. The black line and grey shade show the fitted linear regression and the standard error of estimate, respectively. **b.** Boxplot of the width/length ratio (lacrimal width/skull length). **c.** Principal Component Analysis (PCA) showing the distribution of individual specimens. **d.** Bivariate plot of the first dimension of the PCA and skull length. The black line and grey shade show the fitted linear regression and the standard error of estimate, respectively.

skull (width/length ratio), *M. t. artata* shows a smaller ratio in comparison with *M. t. centralis* and *M. t. tridactyla* (Fig. 3b).

The first dimension of the PCA explains 50.7%, whereas the second one explains 11.7% (Fig. 3c; Table 1). The first dimension correlates with skull length (adjusted $R^2 = 0.87$, p-value < 0.001; Fig 3d). The subadult specimen of *M. t. tridactyla* (NRM 586631) has a skull length that is within the range of values for the adult specimens of *M. t. artata* (Fig. 3a). Similarly, NRM 586631 has the lowest value for the first dimension of the PCA in our sample, and it is closer to the value of several adult specimens of *M. t. artata* than adult specimens of *M. t. tridactyla* (Fig. 3d).

DISCUSSION

The statistical analyses of the cranial measurements suggest that the specimens from north-western Venezuela (*M. t. artata*) are overall smaller than the specimens from Central America (*M. t. centralis*) and specimens from elsewhere in South America (*M. t. tridactyla*). The specimens of *M. t. artata* show shorter and narrower (as measured by the lacrimal width) skulls, and smaller values on the first dimension of the PCA (which correlates with skull length) in comparison with the two other subspecies (Fig. 3). Interestingly, the only subadult specimen in our sample referred to *M. t. tridactyla* (NRM 586631, which comes from the Beni Department in Bolivia) has a skull length within the range of adult specimen of *M. t. artata*, and it has a value on the first PCA dimension that is closer to some adult specimens of *M. t. artata* than to adult specimens of *M. t. tridactyla*.

Some potential qualitative osteological differences have been proposed among the three recognized subspecies. In the description based on a juvenile, Lyon (1906) noted that in *M. t. centralis* the latero-rostral extension of the frontal bones is at the same level that the most rostral extension of the inter-frontal suture, whereas in *M. t. tridactyla* the latero-rostral extension of the frontals is much closer to the most caudal extension of the nasals. Osgood (1912) regarded the fronto-nasal suture condition in *M. t. artata* as somehow intermediate between *M. t. centralis* and *M. t. tridactyla*. However, an examination of the adult specimens from the three subspecies available to us indicates that *M. t. centralis* shows a similar condition to *M. t. artata*. In adult specimens of *M. t. centralis*, the latero-rostral extension of the frontals (red dots in Fig. 4a) is close to the midpoint between the most rostral point of the inter-frontal suture (black dots in Fig. 4a), and the most caudal point of the nasals (blue dots in Fig. 4a).

The fronto-nasal suture morphology in specimens of *M. t. artata* from northwestern Venezuela is similar to the condition seen in the *M. t. centralis* specimens from Panama; but specimens of *M. t. tridactyla* show a position of the latero-rostral extension of the frontals (red dots in Fig. 4a) much closer to the most caudal extension of the nasals (blue dots in Fig. 4a), even in the subadult specimen from Bolivia.

Lyon (1906) also noted that in *M. t. centralis*, the most rostral extension of the squamosal is located closer to the root of the zygomatic than to the most rostral extension of the sphenoid. This condition has also been observed in adult specimens of *M. t. centralis* from Honduras (Mérida Colindres & Cruz Dias 2014). According to Lyon (1906), in *M. t. tridactyla* the rostral extension of the squamosal is located about the midpoint between the root of the zygomatic and the rostral extension of the sphenoid. We notice variation in the squamosal-sphenoid suture morphology among the specimens examined, without clear differences among the three subspecies (Fig. 4b). In the adult specimens of *M. t. centralis*, the most rostral extension of the squamosal (red diamonds in Fig. 4b) is not as closed to the root of the zygomatic (blue diamonds in Fig. 4b), as in the juvenile specimen described by Lyon (1906). Furthermore, the subadult specimen of *M. t. tridactyla* (NRM 586631; Fig. 4b) shows a condition more similar to the one described for the juvenile of *M. t. centralis* (Lyon 1906), suggesting that differences in the relative position of the most rostral extension of the squamosal (red diamonds in Fig. 4b) with respect to the root of the zygomatic (blue diamonds in Fig. 4b) and the most rostral extension of the sphenoid (black diamonds in Fig. 4b) might reflect ontogenetic growth.

Morphological differences in the cranial sutures of populations of *M. tridactyla* have been used to define three subspecies (Lyon 1906, Osgood 1912, Gardner 2007, Gaudin *et al.* 2018). The collection of new specimens from northwestern Venezuela (*M. t. artata*) allows us to better characterize this morphotype and evaluate morphological differences with the other two subspecies. We document a higher morphological variation than previously recognized in the cranial sutures that have been hypothesized to differentiate the subspecies. *M. t. artata* shows smaller cranial dimensions than *M. t. centralis* and *M. t. tridactyla*, and additional analyses integrating data from the genetic variation and from other morphological regions (e.g., internal morphological structures such as the paranasal sinuses; e.g., Billet *et al.* 2017) are required to further evaluate the morphological and genetic differences of the three recognized subspecies.

GIANT ANTEATER FROM NORTHWESTERN VENEZUELA

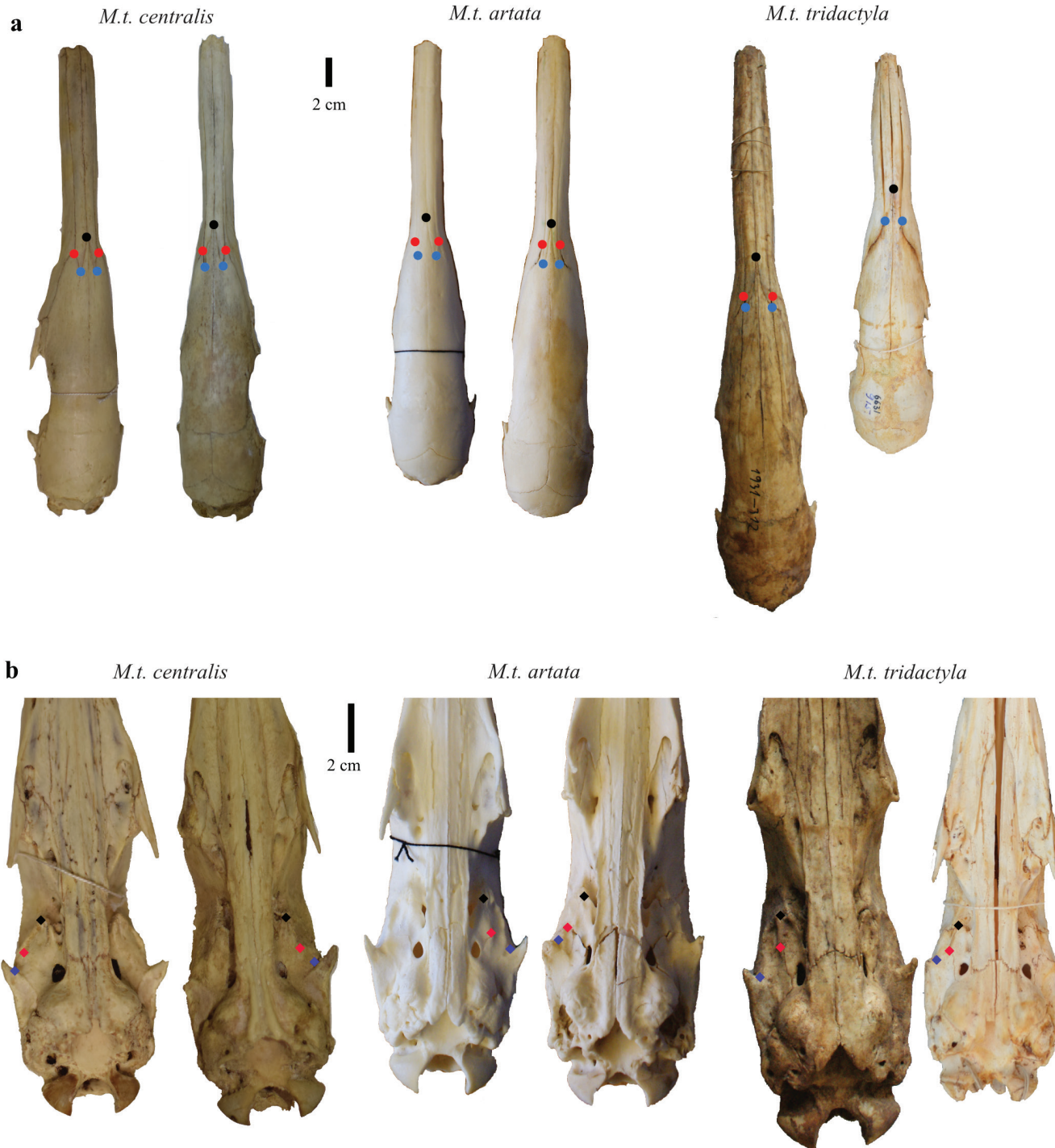


Figure 4. Morphological variation of the cranial sutures in three recognized subspecies of the giant anteater (*Myrmecophaga tridactyla*). **a.** Dorsal view of the skulls showing the relative position the most rostral point of the interfrontal suture (black dot), the most caudal point the nasals (blue dot), and the most latero-rostral extension of the frontals (red dot) in specimens representing the three subspecies of *M. tridactyla*. **b.** Ventral view of the skulls showing the relative position of the most rostral point of the squamosal (red diamond) in relationship with the root of the zygomatic (blue diamond) and the most rostral extension of the alisphenoid (black diamond) in specimens representing the three subspecies of *M. tridactyla*. *M. t. centralis* (left, COSEM-MAS 1033; right COSEM-MAS 1034) from Panama; *M. t. artata* from northwestern Venezuela (left, MBLUZ-0245; right, MBLUZ-M251), and *M. t. tridactyla* (left, ZSM 1931/312, from Paraguay, and right NRM 586631, subadult from Bolivia).

CONCLUSION

The giant anteater (*Myrmecophaga tridactyla*) has a wide geographic distribution in Central and South America, and three subspecies are tentatively recognized (Gardner 2007, Gaudin *et al.* 2018). Of the three subspecies, *M. t. artata* is poorly known and few specimens are available for study in zoological collections (Linares 1998). New specimens from north-western Venezuela allowed us to document the cranial anatomy of *M. t. artata* and evaluate potential morphological differences with the other two recognized subspecies. *M. t. artata* shows overall smaller cranial dimensions for adult specimens in comparison with specimens of *M. t. centralis* and *M. t. tridactyla*, but it is difficult to differentiate the subspecies based on the morphology of the cranial sutures, as previously hypothesized. The specimens of *M. t. artata* studied herein shed light on the cranial morphological variation and overlap among the three recognized subspecies of the giant anteater.

ACKNOWLEDGEMENTS

We would like to thank the following curators and museums for access to the collections under their care: D. Kalthoff (Naturhistoriska riksmuseet, Stockholm), M. Gelang (Naturhistoriska Museum, Gothenburg), G. Veron (Museum National d'Histoire Naturelle, Paris), S. Bock (Museum für Naturkunde, Berlin), A. H. van Heteren (Zoologische Staatssammlung, Munich), M. Schenckel (Zoological Museum, University of Zurich), H. López and C. Cárdenas (Instituto de Ciencias Naturales, Bogotá), A. Cornejo and C. A. Nieto (Instituto Commemorativo Gorgas de Estudios de la Salud, Panama), and G. A. Rivas (Museo de Biología, La Universidad del Zulia). A special thanks to A. Abreu, A. Baran, R. Barboza, M. A. Campos, M. Ortega, D. Revilla, J. Yores and G. A. Rivas for their support in the field work and laboratory. J.D.C. was supported by the Swiss National Science Foundation grants P2ZHP3_174749 and P400PB_186733, and the Helge Ax:son Johnson Stiftelse grant F18-0486. Collecting permits in Venezuela were granted by the Ministerio del Poder Popular para el Ambiente under numbers 5416 (22/10/2008), 665 (10/02/2010) and 1027(24/10/2013). We acknowledge two anonymous reviewers. We thank M. R. Sánchez-Villagra for logistical support of our work in Venezuela, D. Cortés for assistance in the measurements and photographs of specimens of *M. t. centralis* in Panama, and G. Billet, L. Hautier, and S. Ferreira-Cardoso for valuable comments.

REFERENCES

- Billet, G., L. Hautier, B. de Thoisy & F. Delsuc. 2017. The hidden anatomy of paranasal sinuses reveals biogeographically distinct morphotypes in the nine-banded armadillo (*Dasyurus novemcinctus*). *PeerJ* 5: e3593. <https://doi.org/10.7717/peerj.3593>
- Carrillo, J. D., L. E. Sibira & T. R. Barros. 2022. Data from: Cranial anatomy of the giant anteater from north-western Venezuela (*Myrmecophaga tridactyla artata*, Pilosa: Myrmecophagidae)[Dataset]. In: *Anartia*. Zenodo. <https://doi.org/10.5281/zenodo.6652182>
- Casali, D. M., J. E. Dos Santos Júnior, F. R. Miranda, F. Rodrigues Santos & F. Araújo Perini. 2020. Total-evidence phylogeny and divergence times of Vermilingua (Mammalia: Pilosa). *Systematics and Biodiversity*: 1–12. <https://doi.org/10.1080/14772000.2020.1729894>
- Casali, D. M., E. Martins-Santos, A. L. Q. Santos, F. R. Miranda, G. A. B. Mahecha & F. A. Perini. 2017. Morphology of the tongue of Vermilingua (Xenarthra: Pilosa) and evolutionary considerations. *Journal of Morphology* 278: 1380–1399. <https://doi.org/10.1002/jmor.20718>
- Chacón Pacheco, J., J. Figel, C. Rojano, J. Racero-Casarrubia, E. Humanez-López & H. Padilla. 2017. Actualización de la distribución e identificación de áreas prioritarias para la conservación de una especie olvidada: el hormiguero gigante en Colombia. *Edentata*. <https://doi.org/10.2305/IUCN.CH.2017.Edentata-18-1.3.en>
- Dryden, I. L. & K. V. Mardia. 1993. Multivariate Shape Analysis. *The Indian Journal of Statistics, Series A* 55: 460–480.
- Ferreira-Cardoso, S., G. Billet, P. Gaubert, F. Delsuc & L. Hautier. 2020a. Skull shape variation in extant pangolins (Pholidota: Manidae): allometric patterns and systematic implications. *Zoological Journal of the Linnean Society* 188: 255–275. <https://doi.org/10.1093/zoolinnean/zlz096>
- Ferreira-Cardoso, S., P.-H. Fabre, B. de Thoisy, F. Delsuc & L. Hautier. 2020b. Comparative masticatory myology in anteaters and its implications for interpreting morphological convergence in myrmecophagous placentals. *PeerJ* 8: e9690. <https://doi.org/10.7717/peerj.9690>
- Gardner, A. 2007. Suborder Vermilingua Illiger. 1811. pp. 168–177. In: Gardner, A. (ed.). *Mammals of South America. Volume 1: marsupials, xenarthrans, shrews, and bats*. Chicago: University of Chicago Press.
- Gaudin, T. J., P. Hicks & Y. Di Blanco. 2018. *Myrmecophaga tridactyla* (Pilosa: Myrmecophagidae). *Mammalian Species* 50: 1–13. <https://doi.org/10.1093/mspecies/sey001>
- Gibb, G. C., F. L. Condamine, M. Kuch, J. Enk, N. Moraes-Barros, M. Superina, H. N. Poinar & F. Delsuc. 2016. Shotgun mitogenomics provides a reference phylogenetic framework and timescale for living xenarthrans. *Molecular Biology and Evolution* 33: 621–642. <https://doi.org/10.1093/molbev/msv250>
- Gray, J. E. 1821. On the natural arrangement of vertebrate animals. *London Medical Repository* 15: 296–310.

- Gray, J. E. 1825. An outline of an attempt at the disposition of the Mammalia into tribes and families with a list of the genera apparently appertaining to each tribe. *Annals of Philosophy* 10: 337–344.
- Hayssen, V. 2011. *Tamandua tetradactyla* (Pilosa: Myrmecophagidae). *Mammalian Species* 43: 64–74. <https://doi.org/10.1644/875.1>
- Hirschfeld, S. E. 1976. A new fossil anteater (Edentata, Mammalia) from Colombia, S. A. and evolution of the Vermiliongua. *Journal of Paleontology* 50: 419–432.
- Husson, F., J. Josse, S. Le & J. M. Maintainer. 2020. Package “FactoMineR.” *Multivariate Exploratory Data Analysis and Data Mining*. Available from: <http://factominer.free.fr> (November 18, 2021)
- Josse, J. & F. Husson. 2016. missMDA: a package for handling missing values in multivariate data analysis. *Journal of Statistical Software* 70. <https://doi.org/10.18637/jss.v070.i01>
- Linares, O. J. 1998. *Mamíferos de Venezuela*. Caracas: Sociedad Conservacionista Audubon de Venezuela, 691 pp.
- Linnaeus, C. 1758. *Systema naturae per regna tria naturae, secundum classes, ordines, genera, species, cum characteribus, differentiis, synonymis, locis*. Editio Decima, reformata. Holmiae: Laurentius Salvius. 1: iv + 823 + [i] pp.
- Lyon, M. W. 1906. Description of a new species of great anteater from Central America. *Proceedings of the United States National Museum* 31: 569–571. <https://doi.org/10.5479/si.00963801.31-1496.569>
- Mérida Colindres, J. E. & G. A. Cruz Dias. 2014. Confirmación de la presencia del oso hormiguero gigante *Myrmecophaga tridactyla centralis* (Xenarthra: Myrmecophagidae) en la Reserva Biósfera Río Plátano, Departamento de Gracias a Dios, Honduras, con descripción y comentarios sobre su estatus taxo. *Edentata* 15: 9–15. <https://doi.org/10.5537/020.015.0112>
- Miranda, F., A. Bertassoni & A. M. Abba. 2014. *Myrmecophaga tridactyla*. *The IUCN Red List of Threatened Species 2014*, e.T14224A47441961. <https://dx.doi.org/10.2305/IUCN.UK.2014-1.RLTS.T14224A47441961>
- Miranda, F. R., D. M. Casali, F. A. Perini, F. A. Machado & F. R. Santos. 2018. Taxonomic review of the genus *Cyclopes* Gray, 1821 (Xenarthra: Pilosa), with the revalidation and description of new species. *Zoological Journal of the Linnean Society* 183: 687–721. <https://doi.org/10.1093/zoolinnean/zlx079>
- Naples, V. L. 1999. Morphology, evolution and function of feeding in the giant anteater (*Myrmecophaga tridactyla*). *Journal of Zoology* 249: 19–41. <https://doi.org/10.1111/j.1469-7998.1999.tb01057.x>
- Navarrete, D. & J. Ortega. 2011. *Tamandua mexicana* (Pilosa: Myrmecophagidae). *Mammalian Species* 43: 56–63. <https://doi.org/10.1644/874.1>
- Osgood, W. H. 1912. Mammals from western Venezuela and eastern Colombia. *Field Museum of Natural History, Zoology Series* 7: 1–48.
- Pittier, H. & H. H. Tate. 1932. Sobre fauna venezolana. *Boletín de la Sociedad Venezolana de Ciencias Naturales* 7: 249–278.
- R Core Team. 2021. *R: A language and environment for statistical computing*.
- Redford, K. H. 1987. Ants and termites as food. Patterns of mammalian myrmecophagy. pp. 349–399. In: *Current Mammalogy*. New York: Plenum Press.
- Reeve, E. C. R. 1940. Relative growth in the snout of Anteaters. A study in the application of quantitative methods to systematics. *Proceedings of the Zoological Society of London* A110: 47–80. <https://doi.org/10.1111/j.1469-7998.1940.tb08460.x>
- Rodrigues, F. H. G., Í. M. Medri, G. H. B. De Miranda, C. Camilo-Alves & G. Mourão. 2008. Anteater behavior and ecology. pp. 257–268. In: Vizcaíno, S. F. & W. Loughry (eds.). *The Biology of the Xenarthra*. Gainsville: University Press of Florida.
- Rovereto, C. 1914. Los estratos araucanos y sus fósiles. *Anales del Museo Nacional de Historia Natural de Buenos Aires* 25: 1–249.
- Wetzel, R. M. 1975. The species of *Tamandua* Gray (Edentata, Myrmecophagidae). *Proceedings of the Biological Society of Washington* 88: 95–112.